nature microbiology

ARTICLES

https://doi.org/10.1038/s41564-018-0257-9

Recovery of gut microbiota of healthy adults following antibiotic exposure

Albert Palleja[1,2,23], Kristian H. Mikkelsen[3,23], Sofia K. Forslund[4,5,6,7,8,23], Alireza Kashani[1,9], Kristine H. Allin[1,10], Trine Nielsen[1], Tue H. Hansen[1], Suisha Liang[11,12], Qiang Feng[11,12], Chenchen Zhang[11,12], Paul Theodor Pyl[1], Luis Pedro Coelho[8], Huanming Yang[11,12,13], Jian Wang[11,12,13], Athanasios Typas[8,14], Morten F. Nielsen[3], Henrik Bjorn Nielsen[2], Peer Bork[5,8,15,16], Jun Wang[17,18,19,20], Tina Vilsbøll[3], Torben Hansen[1,21], Filip K. Knop[1,3,22*], Manimozhiyan Arumugam[1*] and Oluf Pedersen[1*]

To minimize the impact of antibiotics, gut microorganisms harbour and exchange antibiotics resistance genes, collectively called their resistome. Using shotgun sequencing-based metagenomics, we analysed the partial eradication and subsequent regrowth of the gut microbiota in 12 healthy men over a 6-month period following a 4-day intervention with a cocktail of 3 last-resort antibiotics: meropenem, gentamicin and vancomycin. Initial changes included blooms of enterobacteria and other pathobionts, such as *Enterococcus faecalis* and *Fusobacterium nucleatum*, and the depletion of *Bifidobacterium* species and butyrate producers. The gut microbiota of the subjects recovered to near-baseline composition within 1.5 months, although 9 common species, which were present in all subjects before the treatment, remained undetectable in most of the subjects after 180 days. Species that harbour β-lactam resistance genes were positively selected for during and after the intervention. Harbouring glycopeptide or aminoglycoside resistance genes increased the odds of de novo colonization, however, the former also decreased the odds of survival. Compositional changes under antibiotic intervention in vivo matched results from in vitro susceptibility tests. Despite a mild yet long-lasting imprint following antibiotics exposure, the gut microbiota of healthy young adults are resilient to a short-term broad-spectrum antibiotics intervention and their antibiotics resistance gene carriage modulates their recovery processes.

Human gut microbiota form complex, balanced ecosystems[1]. Perturbations of these biota may drive infections[2], obesity[3,4], diabetes[5–7] and inflammatory[8] and neurological disorders[9]. Rodent and human studies have shown that fecal transplants[10], prebiotics[11], probiotics[12] and antibiotics[13], for example, can alter the gut microbiota and improve host health. An estimated increase in life expectancy of 2–10 years is attributable to antibiotics[14]. However, early-life exposure to antibiotics (especially macrolides) has also been associated with metabolic, inflammatory and neurological impairments both in animal models[15–17] and in observational human studies[18–22].

When exposed to antibiotics, microbial communities respond not only by changing their composition, but also by evolving, optimizing and disseminating antibiotic resistance genes (ARGs), collectively forming resistomes[23]. The human gut microbiota is considered a reservoir for ARGs where members exchange these genes, thereby propagating resistance[24]. The development and spread of microbial antibiotic resistance is a serious health concern given that previously reliable antibiotics now fail. The intestinal microbiota from subjects in different countries harbour different ARG repertoires, reflecting the local usage patterns of antibiotics in healthcare and food production[25]. However, only a few studies have characterized the effects of particular antibiotic regimens on the gut ecosystems of individuals with respect to the associated resistomes. In a longitudinal 16S ribosomal RNA gene amplification and shotgun metagenomics study of children receiving macrolides or penicillins

[1]Novo Nordisk Foundation Center for Basic Metabolic Research, Faculty of Health and Medical Sciences, University of Copenhagen, Copenhagen, Denmark. [2]Clinical-Microbiomics A/S, Copenhagen, Denmark. [3]Center for Diabetes Research, Gentofte Hospital, University of Copenhagen, Hellerup, Denmark. [4]Experimental and Clinical Research Center, Charité-Universitätsmedizin Berlin and Max Delbruck Center for Molecular Medicine, Berlin, Germany. [5]Max Delbruck Center for Molecular Medicine in the Helmholtz Association, Berlin, Germany. [6]Charité-Universitätsmedizin Berlin , Freie Universität Berlin Humboldt-Universität zu Berlin and Berlin Institute of Health, Berlin, Germany. [7]Berlin Institute of Health, Berlin, Germany. [8]Structural and Computational Biology Unit, European Molecular Biology Laboratory, Heidelberg, Germany. [9]Danish Diabetes Academy, Odense, Denmark. [10]Department of Clinical Epidemiology, Bispebjerg and Frederiksberg Hospital, Copenhagen, Denmark. [11]BGI-Shenzhen, Shenzhen, China. [12]China National GeneBank, BGI-Shenzhen, Shenzhen, China. [13]James D. Watson Institute of Genome Sciences, Hangzhou, China. [14]Genome Biology Unit, European Molecular Biology Laboratory, Heidelberg, Germany. [15]Molecular Medicine Partnership Unit, University of Heidelberg and European Molecular Biology Laboratory, Heidelberg, Germany. [16]Department of Bioinformatics, Biocenter, University of Würzburg, Würzburg, Germany. [17]iCarbonX, Shenzhen, China. [18]Beijing Advanced Innovation Center for Food Nutrition and Human Health, College of Food Science and Nutritional Engineering, China Agricultural University, Beijing, China. [19]Department of Biology, University of Copenhagen, Copenhagen, Denmark. [20]State Key Laboratory of Quality Research in Chinese Medicine/Macau Institute for Applied Research in Medicine and Health, Macau University of Science and Technology, Avenida Wai Long, Taipa Macau, China. [21]Faculty of Health Sciences, University of Southern Denmark, Odense, Denmark. [22]Department of Clinical Medicine, Faculty of Health and Medical Sciences, University of Copenhagen, Copenhagen, Denmark. [23]These authors contributed equally: Albert Palleja, Kristian H. Mikkelsen, Sofia K. Forslund. *e-mail: filipknop@dadlnet.dk; arumugam@sund.ku.dk; oluf@sund.ku.dk

(β-lactams), we found decreased diversity and enriched ARG carriage from the exposure, more so in the former than the latter[18]. Two previous 16S rRNA gene amplification-based studies performed in one cohort demonstrated how treating healthy individuals with a single common antibiotic (for example, clindamycin, ciprofloxacin, amoxicillin or minocycline) led to an enrichment of ARGs (imputed based on taxonomic composition) and long-lasting compositional effects on the microbiota, including depletion of butyrate-producing species[26,27]. Another 16S rRNA gene study reported that a seven-day treatment with vancomycin caused profound changes in the microbiota, whereas a seven-day amoxicillin treatment did not[28]. In contrast, a recent single-antibiotic study reported reduced microbial diversity after a three-day amoxicillin treatment[29]. Finally, a study using shotgun metagenomic data suggested that the effects of cefprozil (a β-lactam) on the gut microbiota depended on its initial state[30], reconciling previously divergent results. Antibiotic resistance genes undetected at baseline were found after a seven-day treatment with the antibiotic[30]. However, the effects of a combinatorial multiple-antibiotic treatment on the microbiota and the role of ARGs in gut microbial persistence have not been studied so far.

Recently, we conducted an intervention in 12 healthy men who underwent prospective eradication of the gut microbiota through a combination of three broad-spectrum bactericidal antibiotics (vancomycin, gentamicin and meropenem) during a single four-day course and investigated the effects on host metabolism[31]. This multidrug cocktail is a modified version of prophylactic antibiotic protocols from intensive care units[32] and includes antibiotics given to patients with infections by multidrug-resistant bacteria. In the present study, using shotgun metagenomics on stool samples collected before and at four different time points over a period of six months after treatment, we tracked the process of eradication, partial survival, gradual regrowth and re-establishment of these gut microbial communities. Using a metagenomic species approach[33], we link individual ARGs of the resistome to their carrier taxa, assessing how the ARG repertoire of intestinal microorganisms helps or hinders them during survival and recolonization.

Results

Overall composition of gut microbiota of young healthy adults recovers from a broad-spectrum antibiotic exposure. We characterized the gut microbial composition of the 12 study subjects using species-level metagenomic operational taxonomic units (mOTUs)[34]. Using samples collected at baseline (D0), immediately after antibiotic treatment (4 d after baseline; D4) and at three further time points (8, 42 and 180 d after baseline; D8, D42 and D180, respectively), we traced the eradication and recovery of gut microbial species by ecological alpha and beta diversity measures. The gut microbial alpha diversity of our subjects recovered within six months of the intervention (Fig. 1). By D4, immediately after intervention, both the species richness and Shannon diversity were dramatically reduced compared to D0 (two-sided Wilcoxon signed-rank test; false discovery rate (FDR)-adjusted P values (q) = 0.0098 and q = 0.0065, respectively). However, despite the broad-spectrum nature of the intensive antibiotic treatment, full eradication was not achieved and numerous species were detectable by D4 (Fig. 1a). By D8, the gut microbiota still exhibited reduced richness, but Shannon diversity had significantly increased (Fig. 1b; two-sided Wilcoxon signed-rank test; q = 0.0065), suggesting that the surviving microorganisms started recovery by regrowing more evenly. Thereafter, both richness and Shannon diversity were gradually regained during the six-month follow-up (as measured at D42 and D180). Interestingly, although we observed no significant differences in Shannon diversity between D0 and D180, the species richness remained significantly lower by D180 (two-sided Wilcoxon signed-rank test; q = 0.011), suggesting that some microorganisms that were originally present may have been permanently lost or severely depleted due to the treatment.

In line with the alpha diversity measures, principal coordinate analysis based on Bray–Curtis dissimilarities demonstrated that gut microbial compositions immediately after treatment (D4 and D8) had profound differences from D0, but gradually returned towards their initial composition (Fig. 2a). To analyse the full compositional changes after antibiotic perturbation beyond the first two principal coordinates, we compared the perturbed samples to their corresponding samples at D0 using Bray–Curtis dissimilarities. To verify whether these observed changes were more severe than expected over time in the absence of antibiotics, we also compared the Bray–Curtis dissimilarities between same-donor samples in our cohort to Bray–Curtis dissimilarities between same-donor samples with comparable sampling intervals in two control populations[35,36]. Compared to D0 samples, D4 and D8 showed very high compositional differences (median values 0.98 and 0.95, respectively), indicating drastic changes in the microbiome composition immediately post-treatment (Fig. 2b). These differences were significantly larger than same-donor differences in the control populations (two-sided Wilcoxon rank-sum test, $q < 0.001$). By D42 and D180, the communities still exhibited compositional differences from D0, but at a significantly lower magnitude (median values 0.70 and 0.64, respectively). These differences were still significantly larger than same-donor differences at even larger time separations in control populations (Fig. 2b; two-sided Wilcoxon rank-sum test, $q < 0.05$). However, the compositional differences between D42 and D180 samples were not significantly different from the variation seen over comparable durations in control populations (Fig. 2b, rightmost panel; two-sided Wilcoxon rank-sum test; US Human Microbiome Project (HMP) dataset, time interval > 100 d, $P = 0.10$; Voigt dataset, time interval > 300 d, $P = 0.57$) suggesting that the gut microbiota had reached a stable composition by D42.

Specific microbial taxonomic changes during recovery and recolonization. We investigated which microorganisms became extinct or survived after the treatment, which microorganisms colonized the gut de novo and which microorganisms were lost permanently by following the changes in the relative abundance of individual microbial species over time. By D8, 4 days post-intervention, the relative abundances of 50 species had significantly changed (two-sided Wilcoxon signed-rank test adjusted for compositionality, $q < 0.05$). There was an enrichment of low-abundance commensals like *Escherichia coli, Veillonella* spp., *Klebsiella* spp., *E. faecalis* and *F. nucleatum* (Supplementary Fig. 1 and Supplementary Table 1), indicating a major ecological change. We also observed a depletion of other commensals, particularly butyrate producers, such as *Faecalibacterium prausnitzii*, *Roseburia hominis*, *Anaerostipes hadrus*, *Coprococcus* spp. and *Eubacterium* spp. This replicates reported decreases of short-chain fatty acid producers under antibiotic treatment[27,28].

By D42, none of the species whose relative abundance differed significantly between D0 and D8 exhibited significant differences, suggesting that most of the dominant microorganisms of the human gut had regrown. Some of the previously blooming species, including *Klebsiella* spp., *Megasphaera micronuciformis*, *E. faecalis* and *F. nucleatum*, were no longer detectable. Others, such as *E. coli* and *Veillonella* spp., remained but returned to D0 levels, so that by the end of the observational period they were not particularly elevated. *Clostridium* spp. were generally undetectable pre-intervention but significantly increased in their relative abundance by D42 (two-sided Wilcoxon signed-rank test after adjusting for compositionality, $q < 0.05$) (Supplementary Fig. 1 and Supplementary Table 1). These species are known to form endospores under unfavourable conditions, reviving when environmental conditions are once again favourable[37]. This may have provided them with an advantage in our clinical setup, with spores reviving on sensing an emptier gut and effectively colonizing the gut after intervention. Specifically,

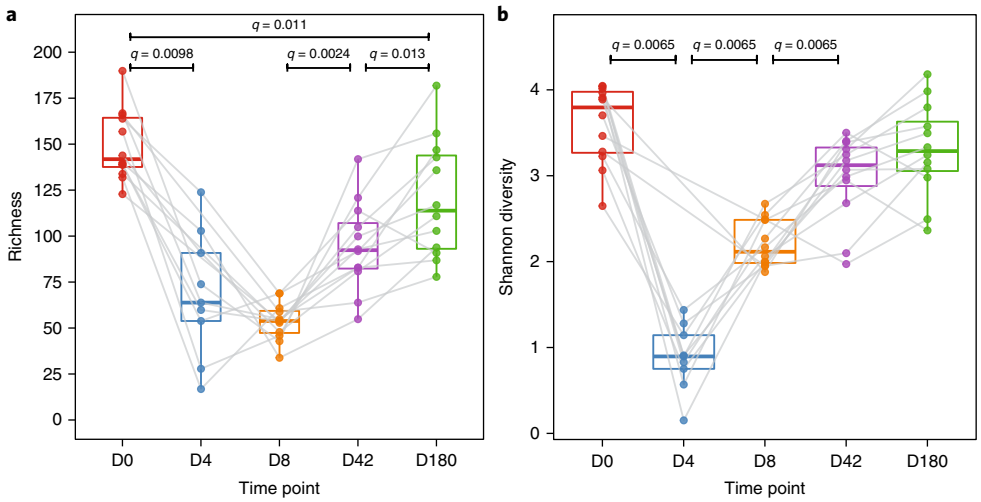

Fig. 1 | Gut microbial diversity recovers after a broad-spectrum antibiotic intervention. a,**b**, Microbial richness (**a**) and Shannon diversity (**b**) based on mOTU relative abundances. The boxplots represent the diversity measures for the 12 volunteers (centre line, median; box limits, first and third quartiles; whiskers, 1.5 × interquartile range), which are also represented as points connected across time by grey lines. Samples are coloured according to time point ($n = 57$). The FDR-adjusted P values are shown between consecutive time points (two-sided Wilcoxon signed-rank test).

Clostridium bolteae abundance was significantly increased by D42 (two-sided Wilcoxon signed-rank test after compositionality test, $q = 0.026$) and remained elevated in all 12 subjects on D180 (two-sided Wilcoxon signed-rank tests after compositionality test, $q = 0.052$; Supplementary Figs. 1,2). Finally, some species detected at D0 were not detected again within the study time frame. These included: (1) members of genus *Bifidobacterium* that are considered pathogen-protective and immunostimulatory; (2) butyrate producers such as *Coprococcus eutactus* and *Eubacterium ventriosum* and (3) methane-producing *Methanobrevibacter smithii* associated with the efficient digestion of polysaccharides. These results with regards to compositional changes broadly match expectations from the relative susceptibility to antibiotics of human gut microorganisms from a recent in vitro microbial growth inhibition screen[38] (see Supplementary Analysis, Supplementary Table 4 and Supplementary Fig. 12).

We then investigated taxonomic changes at an increased resolution using metagenomic species[33] (MGSs) derived from the integrated gene catalog (IGC) of 9.9 million gut microbial genes[39]. MGSs include cultured as well as uncultured gut microbial species and provide sub-species-level resolution in some taxonomic groups, as each MGS is probably derived from an independent chromosome[33]. MGS-based analysis confirmed many of the microbial changes observed using mOTUs (Supplementary Fig. 3 and Supplementary Table 1) and highlighted additional changes. It corroborated the post-intervention significant increase of species usually only found at low abundance. Furthermore, it confirmed the depletion of butyrate producers (Supplementary Fig. 3) post-treatment and provided increased sub-species resolution, highlighting eight different MGSs belonging to *F. prausnitzii*, one to *R. hominis*, three to *Eubacterium* spp. and two to *Coprococcus* spp. as significantly depleted (two-sided Wilcoxon signed-rank test after adjusting for compositionality, $q < 0.05$). Remarkably, only two *F. prausnitzii* strains were able to recover by D180, another six could not recover through the study period (Supplementary Fig. 3), reflecting the different recovery capacities between conspecific strains.

Resistance gene carriage impacts survival and colonization potential of gut microorganisms. We hypothesized that differences in antibiotic resistance potential among microorganisms could explain the differences in their recovery patterns, which involve trends at the species level (Supplementary Fig. 1) as well as differences between conspecific strains (Supplementary Fig. 3). For this, we updated the ARG annotation of IGC genes[40] to ARG families in the Comprehensive Antibiotic Resistance Database (CARD)[41] and the ResFams[42] database. By mapping metagenomic reads to IGC, we estimated the abundance of known ARGs against β-lactams (parent class of meropenem; note that several β-lactamases cannot cleave carbapenems[43]), aminoglycosides (parent class of gentamicin), glycopeptides (parent class of vancomycin) and all other antibiotic classes, which were grouped for comparison. We conducted the analysis at the antibiotic class level as existing ARG annotation is frequently incomplete, whereas cross-resistance between structurally similar antibiotics is common and likewise incompletely annotated. We further quantified multidrug efflux pumps (MEPs), which could potentially confer unspecific multidrug resistance. Antibiotic resistance genes against β-lactams and aminoglycosides were not significantly altered from D0 abundances (Fig. 3). Our results were robust to the choice of ARG database (see Methods). The larger contribution to the ARG abundance changes that we observed are driven by genes more likely to be chromosomal than located on mobile genetic elements (see Methods). Antibiotic resistance genes against glycopeptides were significantly depleted by D4 and remained so until D8 (Fig. 3; two-sided Wilcoxon signed-rank test, $q < 0.05$). We observed no significant differences when comparing either D42 or D180 to D0. Abundances of MEPs were significantly elevated by D8 (two-sided Wilcoxon signed-rank test, $q < 0.01$) and these were maintained until D42 (two-sided Wilcoxon signed-rank test, $q < 0.05$). By D180, no category showed significant differences when compared to D0 (Fig. 3). Thus, the overall ARG abundance analysis did not show clear temporal patterns that could explain the differences between species and conspecific strains.

Unlike previous gut resistome analyses, our use of the MGS approach[33] enabled us to link ARGs to the MGSs that they belong to. First, we observed that both the MGSs that survived the treatment and the first colonizers often harbour ARGs against multiple antibiotics (Supplementary Figs. 4,5). Second, by using the abundances of MGSs and the abundance of individual ARGs within them, we noted each MGS as either detected or undetected in each study sample and, when detected, we marked those as either resistant or non-resistant to each of the three antibiotics. We then assessed how possession of ARGs affected the chance of survival

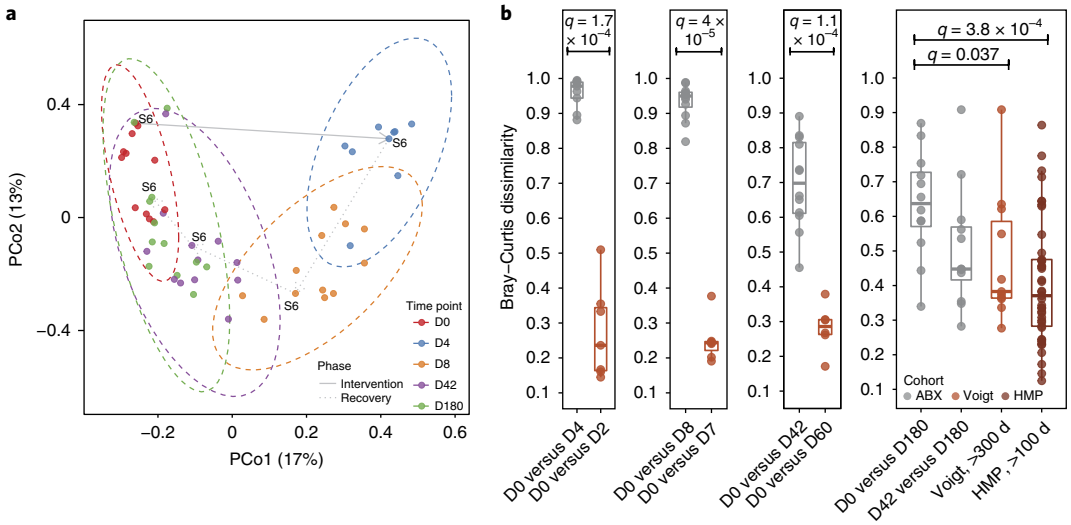

Fig. 2 | Gut microbial composition dramatically changes after broad-spectrum antibiotic intervention but recovers progressively. a, Principal coordinate analysis based on Bray–Curtis dissimilarity between samples, calculated using mOTU relative abundances. Samples are coloured according to time point ($n = 57$) and ellipses represent the 95% confidence interval for each time point assuming a multivariate normal distribution. The grey lines connect samples from the same individual (S6) to denote a representative trajectory followed by the individuals after antibiotic intervention. The variance explained by each axis is stated as a percentage in parentheses. **b**, The boxplots show the Bray–Curtis dissimilarities (as a measure of beta diversity) between same-donor samples from two different time points (centre line, median; box limits, first and third quartiles; whiskers, 1.5 × interquartile range). The four boxplots in the rightmost panel show that the extent of compositional changes between paired samples during the study time (D0 to D180) were significantly different compared to the degree of variation over time observed for paired samples in the Voigt and HMP controls (separated by time spans >300 d and >100 d, respectively) but the compositional changes between D42 and D180 did not differ from the controls. Grey was used to represent the study distances between paired study samples ($n = 57$). Orange and brown was used to represent the distances between paired samples for the Voigt ($n = 35$) and HMP ($n = 82$) datasets, respectively. Two-sided Wilcoxon rank-sum tests were used to test for significant differences between sample distances and FDR-adjusted P values are shown. ABX, antibiotics-treated cohort.

of an MGS (detection at D0 and at a later time point) using Fisher's exact test (see Methods for details). Metagenomic species with β-lactam ARGs had significantly higher odds of survival (odds ratio (OR) = 1.64 (1.24–2.17)) by D8, but this effect decreased at later time points (Fig. 4). In contrast, MGSs with glycopeptide ARGs had significantly decreased chances of survival from D0 to D8 (OR = 0.32 (0.23–0.44)) and D42 (OR = 0.71 (0.60–0.84)), again with the effect weakening over time. This change may be due to the increase of Gram-negative species in the initial time points after treatment, which are naturally resistant to vancomycin without the need for specific ARGs. Strikingly, MGSs with aminoglycoside ARGs exhibited a gradual decrease of survival odds from D0 to D180 (OR = 0.67 (0.48–0.93)). Although we observed a significant enrichment of MEPs by D8 (Fig. 3), MGSs carrying MEPs did not show higher chances of survival. Interestingly, MGSs that were undetected at D0 had significantly higher odds of de novo colonization of the gut ecosystem at a later time point if they carried ARGs against any of the three classes used: aminoglycoside ARGs (OR = 4.32 (2.29–8.57); OR = 1.91 (1.24–2.94); OR = 2.01 (1.39–2.92); for D8, D42 and D180, respectively), β-lactam ARGs (OR = 1.64 (1.12–2.40); OR = 1.40 (1.12–1.77); OR = 1.12 (0.91–1.37), respectively), or glycopeptide ARGs (OR = 2.45 (1.61–3.74); OR = 2.33 (1.86–2.94); OR = 1.33 (1.09–1.62), respectively), although this effect also weakened over time (Fig. 4). We observed the opposite pattern in the long term for MGSs carrying MEPs, suggesting that the possession of more MEPs does not increase the chances of colonizing the gut environment post-treatment (OR = 0.51 (0.35–0.76) and OR = 0.54 (0.38–0.76) for D42 and D180, respectively). The survival and colonization likelihood trends for MGSs harbouring β-lactam and aminoglycoside ARGs were not observed in the control population (HMP same-donor sample pairs with an interval >100 d; Fig. 4), suggesting that MGSs carrying β-lactam ARGs could be positively selected for, whereas species carrying aminoglycoside ARGs here could be negatively selected for. The latter could reflect that aminoglycosides are inactive under anaerobic conditions (as those found in the gut) and are usually administered for local or systemic infections. The trend observed for species carrying glycopeptide ARGs could indicate that, under the present multidrug treatment, carrying vancomycin ARGs may not be beneficial for the survival of a microorganism. This may indicate that these ARGs are not functional and/or are expensive to make (most known vancomycin resistance systems are operons of up to nine genes encoding proteins that build an alternative cell-wall precursor less susceptible to glycopeptide binding[44]), or it could reflect that most of the vancomycin resistance in the gut microbial population is not encoded by ARGs but is due to the overall cell envelope composition. The same trends were observed for carrying glycopeptide ARGs in the control population (HMP; >100 d) but with lower odds (Fig. 4; OR = 0.57 (0.49–0.65) and OR = 1.36 (1.18–1.56) for survival and de novo colonization, respectively). Thus, glycopeptide resistance capacity may be found more frequently in taxa with a generally higher gut turnover. Carrying MEPs significantly increased the chance of MGS survival in the control population (Fig. 4; OR = 1.78 (1.36–2.32)), but we did not observe this pattern in our intensive treatment, suggesting that MEPs were altogether insufficient to provide resistance to our antibiotic cocktail.

We next tested whether ARG families that changed significantly in abundance post-intervention were also enriched within the genomes of species that were enriched post-intervention. Indeed, taxonomic compositional changes predicted the gene-level changes for 65 of 82 families (Supplementary Analysis and Supplementary Table 6). The remaining ARG families may represent cases of genes that are more variably found across conspecific gut strains, or genes that have been carried on mobile elements in the recent evolutionary

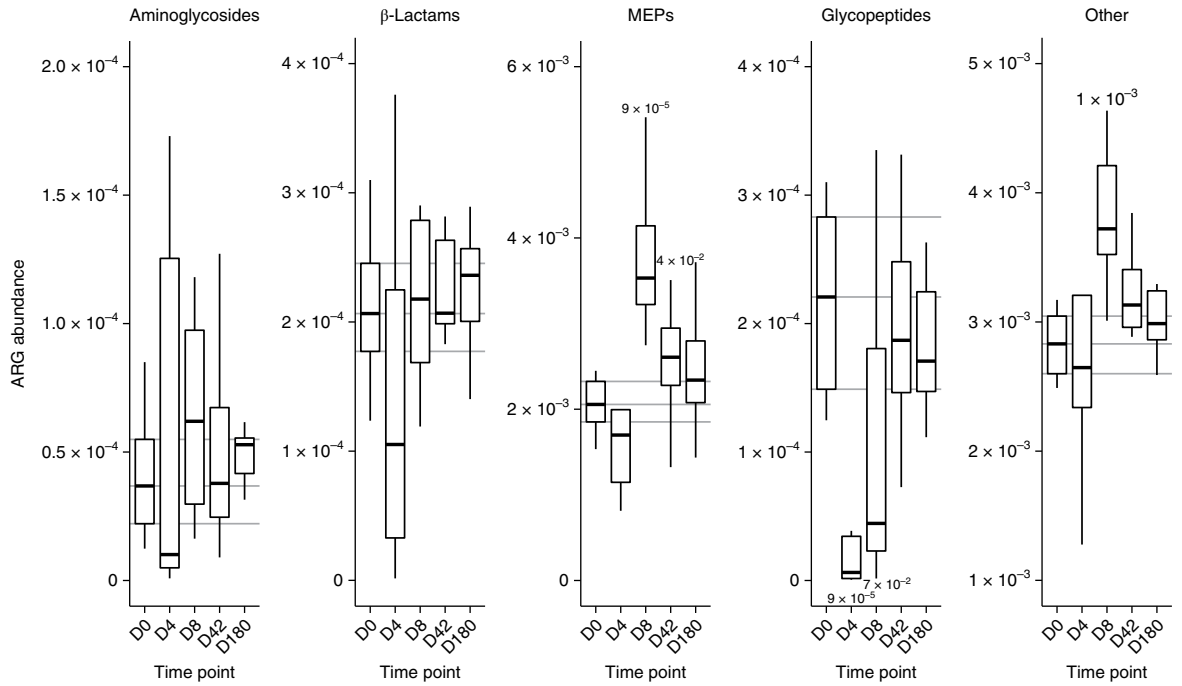

Fig. 3 | Microbial antibiotic resistance potential changes after broad-spectrum antibiotic intervention. Boxplots show the changes in ARG relative abundance (centre line, median; box limits, first and third quartiles; whiskers, 1.5 × interquartile range) throughout the intervention ($n = 57$). These enrichments/depletions are shown for the three drug classes used in the intervention (aminoglycosides, β-lactams and glycopeptides), MEPs and a general category where we pooled ARGs that protect against all other antibiotic classes (other). FDR-adjusted *P* values are shown for the statistically significant enrichments (two-sided Wilcoxon rank-sum test). The grey horizontal lines represent the median and the 25th and 75th percentile values at D0.

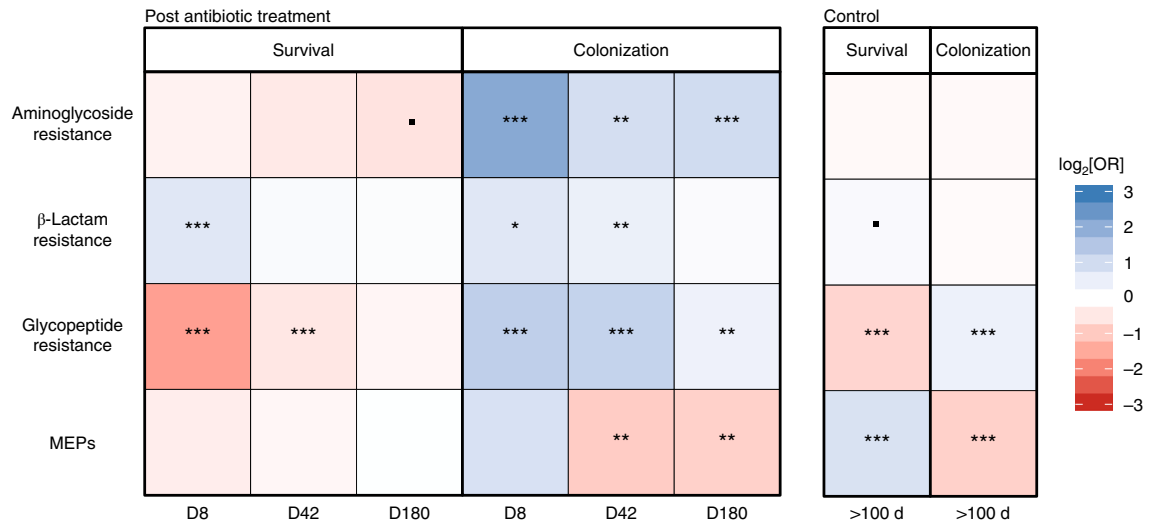

Fig. 4 | Resistance gene carriage impacts the odds of microbial survival and colonization. The left heatmap shows the odds ratio ($\log_2$) of survival and colonization after the intervention of MGSs carrying ARGs to the antibiotics used in the treatment as well as MEPs (for D8, D42 and D180; $n = 48$). The right heatmap shows the same for a control population (HMP; $n = 82$). Asterisks represent statistically significant odds ratios. ***$q < 0.001$; **$0.001 \leq q < 0.01$; *$0.01 \leq q < 0.05$; ▪$0.05 \leq q < 0.1$; Fisher's exact test. Exact FDR *P* values and other details about the statistical test can be found in Supplementary Fig. 4.

past. We note among others that the carpapenem-resistance associated resistance-nodulation-cell division pump AdeJ, characteristic of *Acinetobacter baumannii*[45,46], is detected and elevated after intervention in these samples in the absence of its typical host, suggesting that its genomic carriage in the gut may be wider than previously thought.

Increase of antibiotic resistance functional potential and enrichment of virulence factors following antibiotic exposure. We next investigated whether there were microbial functions that increased in abundance alongside the otherwise usually low-abundance species by D8 and later post-treatment time points. We used previously published annotation of IGC genes[40] to the Kyoto Encyclopedia

of Genes and Genomes (KEGG) database[47], estimating the abundance of KEGG modules and pathways for each sample. The relative abundance of 192 KEGG modules and 64 KEGG pathways changed significantly from D0 to D8 (two-sided Wilcoxon signed-rank test, $q < 0.05$; Supplementary Table 1a). Among the significant modules, 15 represented different efflux pumps, confirming the enrichment of MEP genes identified in our ARG analysis. Five of these efflux complexes included TolC, which is a central component of multiple bacterial efflux pumps that are responsible for exporting numerous and diverse antibiotics, including β-lactams, in both growing and dormant bacteria[48]. It is crucial to note that gene enrichment visible under our study design reflects the fitness of bacterial taxa that carry such genes, which may or may not depend in turn on the thus-enriched genes themselves. The involvement of TolC in efflux pumps extruding bile acids could conceivably impact such fitness, although this cannot be concluded from the present data and remains speculative. Furthermore, we observed an increase in the abundance of transporters including seven bacterial phosphotransferase systems, which catalyse phosphorylation and transportation of a variety of sugars into the cell, allowing microorganisms to maximize the assimilation of available sugars to grow faster in a competitive environment. Remarkably, 27 modules encoding two-component systems, which are basic signalling cascades for responding to environmental perturbations, had significant changes in relative abundance (two-sided Wilcoxon signed-rank test, $q < 0.05$; Supplementary Table 1); this included systems known to respond to glycopeptide (vancomycin/bacitracin) antibiotics in Gram-positive organisms (LiaSR, BceSR, VraSR). Consistent with the increase in enterobacteria and other Gram-negative bacteria at D8, lipopolysaccharide-related features increased, as well as systems for alternative forms of respiration (for example nitrate, tetrathionate and trimethylamine oxide anaerobic respiration). It has been recently shown that the use of alternative electron acceptors, often produced as part of inflammatory response, help enterobacteria to bloom in the human gut[49–52].

By D42, only 41 KEGG modules were significantly different in their relative abundance, including 8 MEPs (6 of which include the TolC gene) and 4 two-component systems, but none of the KEGG modules related to resistance against specific antibiotics (two-sided Wilcoxon signed-rank test, $q < 0.05$; Supplementary Table 1b). By D180, no functional feature from KEGG was significantly different in relative abundance, suggesting that the microbiota recovered to near D0 composition, also with regards to functional potential (Supplementary Table 1c).

Several virulence factors, such as capsule synthesis and type II, III and VI secretion systems (T2SS, T3SS and T6SS; Supplementary Table 1), were also increased by D8, which led us to investigate them further. For this purpose, we used IGC annotations to the Pathosystems Resource Integration Center (PATRIC) database of virulence factors[53] and estimated the abundance of PATRIC functional categories in each sample. Both immediately (D4) and four days (D8) after the treatment there was a strong enrichment of genes involved in quorum sensing. This may be a consequence of selection for bacteria better able to coordinate gene expression under changes in cell density due to significantly reduced microbial density post-treatment. However, our data cannot be used to conclude this. Activities controlled by this system are involved in virulence, pathogenic potential and biofilm formation of microorganisms[54]. By D8, a set of virulence factors were significantly enriched (Fig. 5), including exotoxins, pore-forming toxins and secreted effectors required for invasion or for inhibiting phagosome formation or maturation and allowing intracellular proliferation. In contrast, changes in lipopolysaccharide, capsule formation capacity, fimbriae and pili presumably reflect the increase in enterobacteria, which commonly carry such elements. These observations indicate that the earliest gut colonizers, after suppression of D0 commensals, may be bacteria with pathogenic potential. Despite this initial enrichment of virulence factors after the treatment, these factors were cleared by D42 and did not seem to cause long-term effects in

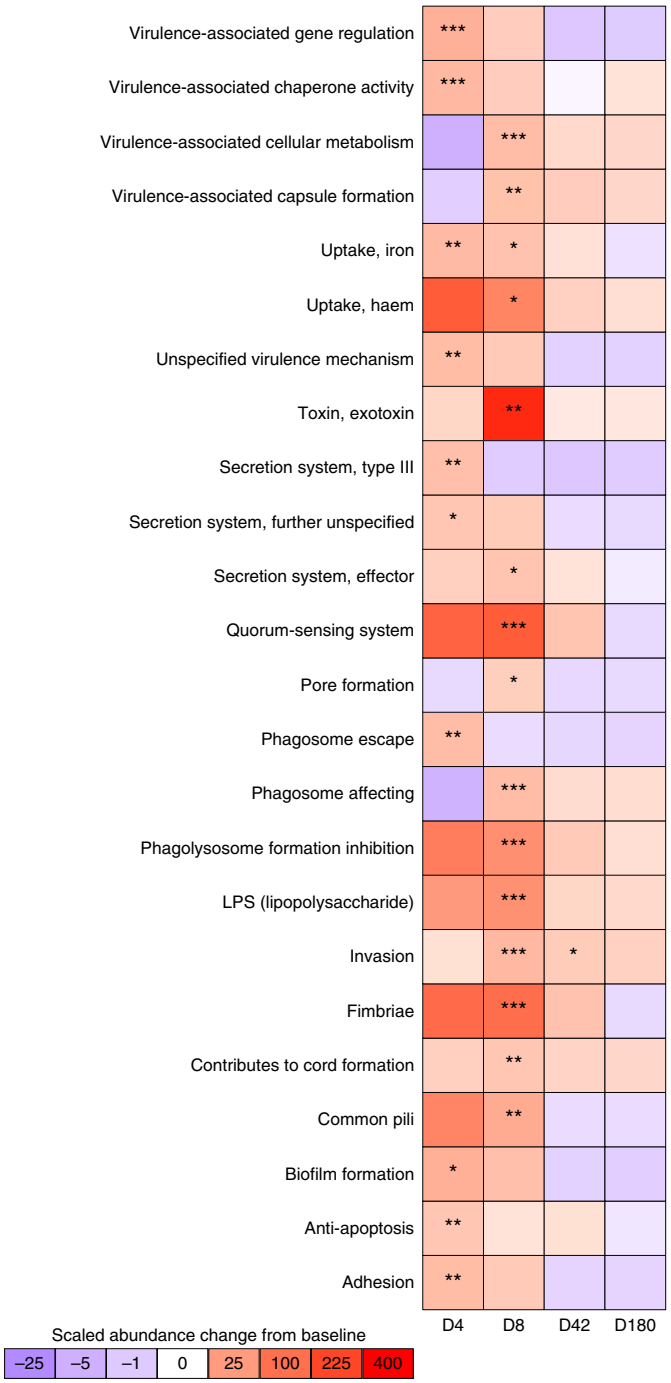

Fig. 5 | Microbial virulence factors are enriched immediately after antibiotic treatment. The heatmap shows differential abundance of genes mapped to each virulence functional category (according to the PATRIC virulence specialty gene set). The mean abundance across all samples ($n = 57$) at each time point was scaled by subtracting D0 abundance and dividing by D0 s.d. The result was then square root-transformed for visibility. Asterisks show significant differences from D0 levels. ***$q < 0.001$; **$0.001 \leq q < 0.01$; *$0.01 \leq q < 0.05$; one-sided Wilcoxon rank-sum test. Exact FDR *P* values and other details about the statistical test can be found in Supplementary Fig. 5.

healthy individuals of this study, which is consistent with what we reported in an earlier study[31].

Discussion

Gut microbiota of young healthy subjects showed resilience and a capacity for recovery from a combinatorial antibiotic treatment designed to maintain prophylaxis on gut microbiota, although some species or strains detectable at D0 remained undetected throughout the rest of the study period. When we compared our metagenomic observations to a recent drug susceptibility screen of diverse gut species, the results were concordant (Supplementary Analysis, Supplementary Table 4 and Supplementary Fig. 12), confirming that we recorded the direct effects of drugs in the gut microbiota. It is important to note that an accurate estimation of the extent of loss of bacteria would require analysis of absolute count data, which could be obtained experimentally through mass-normalized qPCR analysis of samples. Although this was impossible for the present study due to sample availability, it can be undertaken in future follow-up experiments.

Contrary to expectations, we observed no immediate enrichment of ARGs targeted to the antibiotics used in the healthy individuals in this study (Fig. 3). However, four days post-treatment, a specialized community of previously low abundant or undetectable species, alongside ARG and virulence factor enrichment (Figs. 3,5 and Supplementary Fig. 4) arose, whereas short-chain fatty acid producers, particularly butyrate producers, were depleted as reported in earlier studies[27,28]. The increase in the abundance of MEP genes and microbial structural elements (for example lipopolysaccharide, pili, fimbriae, among others) presumably reflects the taxonomical changes observed post-treatment, as many of these systems are part of the core genomes of Enterobacteriaceae spp., which increased after the treatment (for example, *E. coli* and *Klebsiella* spp.). Other virulence elements (for example, T2SS, T3SS, T6SS, capsules and exotoxins) seemed to exhibit enrichment beyond what these taxonomic shifts imply, as they were present only in some virulent strains of Enterobacteriaceae spp. and/or other unrelated pathobiont species.

Interestingly, *Clostridium* spp. were particularly likely to colonize after the antibiotic intervention, perhaps having survived as spores. This is relevant as *Clostridium difficile* infections are associated with the use of broad-spectrum antibiotics in acute care settings, which reduce host resistance to colonization and expansion of this pathogen[55]. Fecal microbiota transplantation successfully treats recurrent *C. difficile* infections by reconstituting the normal microbiota homeostasis and thus breaking the infection recurrence cycle[56]. Future drug development to minimize antibiotic-induced gut dysbiosis should target the *Clostridium* spore-germination process and increase the abundance of beneficial species with direct colonization resistance such as *Bifidobacterium* spp., which were depleted by our intervention. We validated and extended the results of a previous report[30], where *C. bolteae* was enriched after a single course of a β-lactam antibiotic. Thus, we hypothesize that rather than being a direct marker for autism[57–59], liver transplant rejection in rats[60], or low diversity[61] as previously suggested, *C. bolteae* might be a marker of general β-lactam and/or antibiotic-induced dysbiosis, as patients with these disorders or conditions are likely to be overexposed to antibiotics. Consistently, *C. bolteae* is particularly resistant to β-lactams in vitro, compared to other firmicutes[38]. This should be further analysed with an appropriate experimental design that enables disentangling the effects of antibiotic uptake from those of the disorders themselves on the gut microbiota.

By combining shotgun metagenomics with a quantitative metagenomic species approach, we tested whether antibiotic resistance potential modulates gut microbial recovery following antibiotic treatment. Microorganisms that harbour β-lactam ARGs exhibited initially increased odds of survival and de novo colonization post-treatment. Species harbouring β-lactam, but not aminoglycoside ARGs, were possibly positively selected for by our intervention, which is consistent with the stronger action of β-lactams against enteric bacteria and in anaerobic conditions. Strikingly, while microorganisms carrying glycopeptide ARGs exhibited increased odds of de novo colonization, they had decreased odds of survival through the intervention, possibly reflecting that such resistance mechanisms may be inactive or too energy- and time-consuming to be activated during the short course of a multidrug antibiotic challenge. We cannot exclude interactions between the three administered drugs that may partially mask their effects or render their resistance mechanisms obsolete. Moreover, as we rely on databases of curated ARG families, we cannot rule out the possibility that the enrichment of ARG families may be biased by the extent to which antibiotic resistance has been characterized in different organisms. Many of the gene-level findings that we report are due to the taxonomic shifts (Supplementary Analysis and Supplementary Tables 5,6); that is, they could be considered as gene/functional-level projections of taxonomic shifts. Although we hypothesize that these shifts in functional potential may provide a fitness advantage to the microorganisms that harbour these functions, metatranscriptomic studies are needed to substantiate or falsify this hypothesis.

In summary, our results demonstrate that the gut microbiota of young, healthy adults are resilient to a four-day broad-spectrum antibiotic treatment, that most of these communities can recover to their D0 composition and that the resilience/recovery patterns of individual species are modulated by ARG carriage. Further studies are needed to verify whether the human gut microbiota is likewise resilient to multiple antibiotic exposures over prolonged periods and whether these results hold in children with an immature gut microbiota or in elderly people with an age-related decline in immune competence and perturbed intestinal microbiota.

Methods

Study volunteers and antibiotic exposure. Fecal samples were taken from 12 healthy Caucasian males, aged between 18 and 40 yr with an average age of 23.4 yr (s.d. = 5.3 yr) at the start of the study, glycated haemoglobin A1c below 43 mmol mol^{-1} (<6.1%) and with normal bowel function (1–3 bowel movements per day). The exclusion criteria included: any use of antibiotics 6 months before inclusion; BMI below 18.5 kg m^{-2} or above 25 kg m^{-2}; smoking; abnormal serum/plasma levels of electrolytes, lipids, creatinine, liver enzymes (alanine transaminase, aspartate aminotransferase, alkaline phosphatase), thyroid stimulating hormone or haemoglobin; any current or existing disease in the gastrointestinal system or family history of inflammatory bowel disease or diabetes; lactose intolerance or coeliac disease; allergy against the antibiotics used in this study and the use of medication that could not be paused during the study period. In addition to a screening visit, the study design encompassed five study visits (D0, D4, D8, D42 and D180) and a four-day broad-spectrum antibiotic intervention consisting of once-daily administration of 500 mg meropenem, 500 mg vancomycin and 40 mg gentamicin dissolved in apple juice and ingested orally. This cocktail is a modified version of a protocol used in intensive care units[32] and is designed to eradicate as many gut microorganisms as possible without causing direct side effects. None of the three antibiotics are absorbed by the gut mucosa[62–64]. Except keeping the diet unaltered throughout the study period and avoiding yoghurt products on the four days preceding each visit, no dietary regulations were required. The study was approved by the Scientific-Ethics Committee of the Capital Region of Denmark, registered with ClinicalTrials.gov (ID: NCT01633762) and conducted according to the Helsinki Declaration. All the subjects gave informed consent to participate in this study. Data regarding glucose metabolism, and gut and pancreatic hormone secretion have been published previously, alongside further information about the protocol and experimental procedures[31]. The present experiment was conducted only once on the present cohort, with no separate replication cohort at this point.

DNA extraction and shotgun metagenomics sequencing. Stool samples were collected before the treatment at D0 and at D4, D8, D42 and D180. The participants collected fresh stool samples at home that were immediately frozen in their home freezer at −20 °C and delivered to Gentofte Hospital within 36 h of sampling. The samples were transported using insulating polystyrene foam containers with a transport time below 3 h and were stored at −80 °C until DNA extraction. Microbial DNA was extracted from 200 mg frozen stool using the International Human Microbiome Standards standard operating procedure 07 V2[65]. Briefly, bacteria were first subjected to chemical lysis and mechanical lysis by bead-beating; next debris, aromatic compounds, proteins and RNA

were eliminated and finally, DNA was precipitated using alcohol. To enable the extraction of sufficient DNA from seven of the D4 and two of the D8 samples, we modified the DNA extraction procedure by extracting DNA from 3 × 200 mg feces, adding only one-third of the advised amount of both the phosphate buffer and potassium acetate to each sample, and by adding 6 µl RNase (instead of 2 µl) after pooling the three samples. The DNA concentration was determined using a Qubit Fluorometer (Thermo Scientific) and the quality of the extracted DNA was estimated by agarose gel electrophoresis. Three of the samples from D4 repeatedly failed during library construction and were therefore discarded. We optimized the library preparation for six samples at D4 and two samples at D8 (marked by the suffix 'opt' in the Sample ID in Supplementary Table 2). Whole-genome shotgun sequencing was performed on the remaining 57 fecal samples using the Illumina HiSeq 2000 platform under paired-end sequencing (2 × 100 base pairs (bp)). Data generation from the samples through metagenomic sequencing has been shown in a previous report to be fairly robust across multiple replications when standard protocols are applied[36], thus no explicit replication of this step was made. We generated 79.4 ± 18.0 million raw metagenomic reads (7.94 ± 1.8 Gb) per sample. The sequencing depths (in millions of reads) for D0, D4, D8, D42 and D180 samples were 76.5 ± 11.1, 78.1 ± 13.2, 75.6 ± 19.6, 81.2 ± 11.4 and 85.4 ± 26.6, respectively, suggesting that the read depths were not significantly lower in the samples immediately after the intervention. The reads were quality controlled by removing adaptors and by trimming the reads using a quality trimming cut-off of 20 and a minimum read length of 30 bp[66]. On average, 6.8 million reads were filtered out due to adaptor contamination and 0.94 million reads did not pass the trimming criteria. Human DNA reads were removed by screening them against the human genome (version hg19). On average, 0.24 million reads were removed due to human contamination. This resulted in 69.3 ± 8.7, 66.5 ± 13.1, 68.2 ± 15.8, 72.0 ± 12.1 and 79.8 ± 22.6 million high-quality non-human reads per sample for D0, D4, D8, D42 and D180, respectively. Sample information and quality control summary statistics for the reads are shown in Supplementary Table 2.

Taxonomic characterization and ecosystem diversity measures. To generate taxonomic abundance profiles, we used the MOCAT and MOCAT2 software packages[40,66]. Screened high-quality reads were aligned (alignment length cut-off of 45 bp and minimum 97% sequence identity for the option 'screen') to a database consisting of 10 universal single-copy marker genes extracted from 3,496 NCBI reference genomes and 263 metagenomes[34]. We obtained relative abundances for 477 species-level mOTUs. We discarded the low abundance species by removing those that were present in less than two study samples and whose average relative abundance across all samples was lower than 0.01%, resulting in a pruned relative abundance table containing 269 mOTUs. Note that the mOTU annotated here as *C. bolteae* (relevant in the discussion of differential abundance analyses—see Results) has been reclassified as *Lachnoclostridium bolteae* recently[67] and referred to by this name in a previous publication[30].

Based on this table, we calculated species alpha diversity using two measures, the richness per sample by counting the number of mOTUs with non-zero abundance and the Shannon diversity index per sample. The species diversity measures can be affected by the amount of DNA available for sequencing, therefore we analysed whether or not library optimization had any effect on the diversity measures by plotting the richness and Shannon diversity together with the DNA mass per sample (Supplementary Fig. 7). We did not observe any particular pattern for how high or low amounts of DNA in a sample affected by these metrics.

Functional characterization. The high-quality reads were aligned against a combined database (IGChg38 hereafter) consisting of the hg38 release of the human reference genome and the IGC consisting of 9.9 million non-redundant microbial genes[39]. We used bwa mem[68] (version 0.7.15-r1140) with default parameters. The purpose of adding the human genome was to filter out reads that mapped as well or better to some human sequence than to any bacterial gene. The alignments were first filtered to only retain alignments longer than 50 bp with >95% sequence identity. The highest scoring alignment(s) was/were then kept for each read. Alignments were performed separately for paired-end and single-read libraries (single-reads are generated when a corresponding read from the other direction is removed due to the filtering steps mentioned earlier). As IGChg38 is a database predominantly of genes and not genomes, there will be a significant number of read-pairs where one end maps within the gene and the other end maps outside of the gene—either mapping to an adjacent gene or remaining unmapped by falling in the intergenic region. Therefore, we counted a whole read-pair aligning to a gene when (1) both ends from a read-pair mapped to the same gene, (2) only one end from a read-pair mapped to the gene, or (3) a read from the single-read library mapped to the gene. The percentages of read-pairs that mapped to the IGChg38 from D0, D4, D8, D42 and D180 samples were 95.4 ± 1.2, 76.1 ± 21.3, 92.0 ± 5.7, 95.6 ± 1.4 and 95.7 ± 2.4, respectively. In a given metagenomic sample, we estimated the relative abundance of each gene in IGC as follows:

1. Initialize two arrays of read-pair counts with 0 for each entry in IGChg38, U_i and C_i.
2. For each read-pair that maps uniquely to entry i in IGChg38, add 1 to the corresponding count U_i. This results in a uniquely mapped read-pair count for each gene.
3. Set $C_i = U_i$.
4. For each read-pair that mapped to multiple entries (for example, i_1, i_2, i_3, …, i_n) in IGChg38, share it proportionately between these entries based on their abundance estimated from uniquely mapped read-pairs (U_{i1}, U_{i2}, U_{i3}, …, U_{in}). For example, consider a read-pair mapping to multiple entries i_1, i_2,… , i_n. For each j in 1, 2,…, n, the respective C_{ij} entry would be incremented by $U_{ij}/\Sigma_k U_{ik}$.
5. Remove the entries corresponding to human chromosomes.
6. Normalize the counts by gene lengths to obtain abundances.
7. Convert them into relative abundances by dividing individual abundances by the total abundance.

By using the functional annotations of IGChg38 genes provided in the most recent version of the MOCAT2 software[40], we estimated the relative abundance of functional pathways, ARGs and virulence gene families, using the following databases: KEGG[47], CARD[41], ResFams[42] and PATRIC[53]. We summed the abundance of all ARGs providing resistance to any glycopeptide, β-lactam or aminoglycoside (see Results for further reasoning). Genes from the IGChg38 were assigned to a CARD model by applying the CARD RGI software, requiring a hit scoring above the family-specific threshold, with the top hit taken if several were achieved. Similarly, ResFams hits were assigned to genes if no CARD hit was assigned and the score to a ResFams HMM model exceeded the gathering threshold for that model. Of the three ARG models in CARD version 1.1.5, we excluded target loss models (where loss of a gene confers resistance) and protein variant models (for example where known single-nucleotide variants affect antibiotic susceptibility) as ARGs under these models cannot be reliably identified using our analysis pipeline. Instead we used only the CARD homolog models, where under assumptions of curation of the database, the presence of a member of an ARG family is considered a reliable indicator for probable ARG potential. When using the homolog models, we assume that metagenomic reads highly similar to an ARG from a model (having >95% nucleotide similarity) will confer this functional capacity. Although this cannot be fully guaranteed, 95% nucleotide identity is stringent enough to identify genes with very closely related functions, which makes it unlikely that any exceptions will have a significant impact on our reported results. This is also in line with the current state of the art for metagenomic analyses. We tested whether there is a bias introduced by our choice of the ARG database and found that our results on the antibiotics used in this study and on MEPs hold when using the Antibiotic Resistance Gene Database[69], which due to its greater age has different discovery biases (Supplementary Fig. 8). Additionally, we benchmarked our ARG pipeline on three example, well-curated, bacterial genomes. Predicted and manually curated gene assignments (taken from GenBank) are shown in Supplementary Table 3. In brief, of the 154 ARGs assigned by our pipeline to these three genomes, none conflict with the curated annotation and 142 are exact matches or synonyms. The remaining 12/154 are all less specific assignments than the original annotation (for example ABC efflux pump instead of specifically MsbA). Thus, we conclude that the method used here is very conservative and that although false positives must occur, they will be relatively few and we are confident of the results generated with our ARG pipeline. The virulence gene abundances were binned at the level of PATRIC functional descriptors. For differential abundance testing at the microbial functional level, we discarded low abundance KEGG modules and pathways by removing those that were present in fewer than two samples and whose average relative abundance across all samples was lower than 0.01%, resulting in a pruned relative abundance table containing 403 functional modules and 257 pathways.

Identifying metagenomic species. We demonstrated previously how binning co-abundant genes across a series of metagenomic samples enables the construction of MGSs based on a large gene catalog without the need for a reference genome database[33]. In the present study we used the IGC that is more than 2 × larger than the previously used catalog[33]. We built a more complete and accurate collection of such MGSs by grouping co-abundant genes across these 1,267 metagenomes[39], identifying 1,264 MGSs (each comprising at least 700 genes). In our analyses, to estimate the relative abundance of an MGS in a sample, we calculated the median relative abundance of all genes belonging to that MGS in that sample. We then considered the MGS detected if the relative abundance calculated in this way was non-zero (that is, at least half the genes had non-zero abundance). The MGSs were annotated to species level if more than 50% of their genes could be aligned to a RefSeq reference genome at 95% sequence similarity and less than 10% of their genes had an alternative taxonomy. MGSs that could not be annotated at species level were then annotated at the genus level in a similar manner using an 85% sequence similarity requirement. Overall, we were able to map 278 MGSs to the genus and/or species level. We discarded low abundance MGSs by removing those that were present in fewer than two samples and whose average relative abundance across all samples was lower than 0.0001%, resulting in a pruned relative abundance table containing 582 MGSs. Given that we had a sparse relative abundance table with many zero values, specifically for the differential abundance analyses, we set the average relative abundance threshold to 0.01% as with the mOTUs, resulting in a pruned relative abundance table containing 407 MGSs.

Control populations. To determine whether the changes reported here were really associated with the antibiotic treatment and not simply explained by the passage of

time, we employed three different control populations of previously published gut metagenome samples. We downloaded the metagenomes from two cohorts, HMP[35] and another healthy cohort used in a previous report to study the temporal and technical variability of the human microbiome[36] (Voigt; antibiotic-treated samples were excluded), from the European Nucleotide Archive. Eighty-two paired HMP samples from 41 donors sampled at two different time points with time spans >100 d and 35 paired Voigt samples from 7 donors with inter-sample time spans of 2–773 d were processed using MOCAT as described above to produce comparable taxonomic and gene abundance profiles.

Statistical tests. To study the overall effects of antibiotic treatment on the gut microbiota, we determined ecosystem-level metrics such as alpha and beta diversity and used ordination techniques to plot and inspect the relative abundances of the mOTU taxonomic entities resolved. Species richness, Shannon index and Bray–Curtis dissimilarities were computed and principal coordinate analyses were conducted with R using the vegan and ape packages. In amplicon-based studies, where taxonomic resolution varies strongly, a phylogenetic distance measure like UniFrac would be required. Here, as we can achieve a uniform and high resolution through deep shotgun metagenomic data, we instead made use of the Bray–Curtis distance metric, thereby achieving compatibility with previous shotgun metagenomic studies. Samples were rarefied to 14 million inserts using USEARCH software[70] before conducting richness and diversity comparisons. Two-sided paired Wilcoxon signed-rank tests were used to test whether species richness and Shannon diversity were significantly different between paired samples at consecutive time points. Two-sided Wilcoxon rank-sum tests were used to test whether Bray–Curtis dissimilarities between same-donor samples in our study were significantly different to those between same-donor samples with similar time separation in control datasets. We also used two-sided paired Wilcoxon signed-rank tests to determine whether the microbial composition (mOTU and MGS relative abundances) or KEGG functional features (modules and pathways) changed significantly at each sampling time point (D4, D8, D42, D180) compared to D0. For better interpretability of results, we removed mOTU linkage groups without taxonomic annotation before performing differential abundance tests, which resulted in a relative abundance table containing 106 mOTU species. We adjusted the *P* values obtained using the Benjamini–Hochberg FDR-control procedure and reported all changes significant at $q < 0.05$.

Given that the relative abundances of taxa in an ecosystem have to sum to one, relative abundances are compositional data. Differential analysis based on relative abundances is thus susceptible to compositional effects, as an increase in the relative abundance of one taxon will lead to a decrease in the relative abundances of other components[71–73]. To verify whether the observed microbial shifts were real or spurious differences arising due to such effects, we used a previously described compositionality test[74], which verifies whether differences in the relative abundance of a taxon between time points (or groups) were due to a dramatic abundance change in another taxon (Supplementary Table 1). We did not test differences between D0 and D4 because, due to the nature of the intervention, there were pronounced changes during this period in most of the microorganisms, dramatically affecting the relative abundances of the surviving species. That compositional effects will complicate the interpretation of observed changes between these time points can therefore be assumed, even without such a test.

Summing the ARG abundances for each drug, we calculated relative abundances of ARG abundance against β-lactams, aminoglycosides and glycopeptides from all samples at each time point. We also considered MEPs, which can provide broad resistance to the three study antibiotics and an additional category where we pooled all other ARGs for comparison ('others'). Two-sided paired Wilcoxon signed-rank tests were performed to test whether there was a significant enrichment in ARGs against the antibiotic classes used in the intervention at each time point compared to D0 and FDR-adjusted *P* values were reported.

To investigate whether carrying ARGs against the antibiotics used in the study is an advantage for a species in terms of its survival through the intervention or de novo colonization after the intervention, we generated contingency tables for how the survival (or de novo colonization) potential of MGS species changes depending on whether or not they were carrying appropriate ARGs. We compared all post-intervention time points to D0 in this analysis. For instance, to investigate the advantages of carrying aminoglycoside ARGs for survival during the first eight days of the study, this survival versus non-survival contingency table was determined as follows: a) the number of MGSs that were observed in both D0 and D8 (that is, that survived), carrying aminoglycoside ARGs, b) the number of MGSs that were observed in both D0 and D8, not carrying aminoglycoside ARGs, c) the number of MGSs that were observed in D0 but not observed in D8 (that is, that did not survive), carrying aminoglycoside ARGs and d) the number of MGSs that were observed in D0 but not observed in D8, not carrying aminoglycoside ARGs. An MGS was counted multiple times if it occurred in multiple samples, thus we counted the MGS-sample pairs above. Similarly, contingency tables were constructed to investigate the advantages of carrying aminoglycoside ARGs for de novo colonization by counting MGSs that were not observed on D0 but observed on D8 (that is, those that de novo colonized) and MGSs that were observed both on D0 and D8 (that is, those that already existed). Fisher's exact tests were performed on these contingency tables to test whether the chances of survival or de novo colonization are affected by observable ARG carriage. The OR was calculated using the formula OR = ad/bc. Odds ratios are reported in the text with 95% confidence intervals. FDR-adjusted *q* values and odds of survival/colonization were represented in a heatmap. To ensure that our findings were not due to ARGs against one class being found in low-abundant, transient gut microbiota, we used HMP samples to test whether MGSs carrying ARGs against different classes were significantly different in their relative abundance, but we did not find any significant differences (Supplementary Fig. 9).

To assess the enrichment of virulence factors after antibiotic exposure we calculated the mean abundance of virulence factors (summed at the level of functional descriptors) across all samples at each time point and we scaled this number for easier visualization by subtracting D0 abundance and dividing by D0 standard deviation (analogous to a *Z*-score). A one-sided Wilcoxon rank-sum test was used to test whether there was significant enrichment of virulence factors following antibiotic exposure with respect to D0 and FDR-adjusted *P* values were reported. All statistical tests were performed within the R statistical computing environment.

Breakdown of ARG signal by taxonomy. To assess whether or not the changes seen under treatment in antibiotic resistance gene abundance across the cohort can be reduced to contributions from particular clades, we can break down such contributions by counting abundance separately of Co-abundance gene groups/MGSs linked to different clades. Such taxonomic classification is achieved based on the highest similarity of their constituent IGC genes to genomes from the respective clades, under BLASTn analysis. To classify a Co-abundance gene group as belonging to a broader clade (for example a bacterial family), at least 40% of its genes must be most similar to gene variants found within that clade, with no more than 15% most similar to gene variants from another clade. Performing such an analysis for bacterial family, based on the high prevalence of many known ARGs in Enterobacteriaceae, reveals that the aminoglycoside resistance spike at D8 seems driven by this family, whereas the effects on other ARG classes traced are not (Supplementary Fig. 10).

Moreover, although the classification of groups of genes correlated in abundance as either mobile element entities or bacterial chromosomes is still only a partially solved problem, a basic proxy for this classification stems from whether or not such groups are large enough to be chromosomal (MGSs) or too small for this to be the case (Co-abundance gene groups). To assess whether the patterns observed here are driven largely by genes found on chromosomes or on smaller entities such as plasmids, a first check is thus possible by breaking down the respective contribution of these classes of gene groups. Supplementary Fig. 11 shows this analysis, revealing that the bulk of the ARG abundance from each sample traces to groups of correlated genes likely to represent bacterial chromosomes/taxa rather than smaller mobile elements like phages or plasmids.

Robustness to sequencing depth differences. We note that all our samples had a minimum sequencing depth of 17.6 million non-human read-pairs and at least 11.9 million read-pairs were mapped to IGC. Thus, our detection threshold is quite low, on the order of 1 in 10 million. Although we cannot rule out that some specific species were present in a sample below our detection threshold, the overall trends reported in our survival and de novo colonization analysis were not affected by sequencing depth (see Supplementary Fig. 6).

Code availability. For the differential abundance testing, we used a compositionality test available at: https://github.com/apalleja/compositionality_test/. Otherwise standard R packages were used.

Reporting Summary. Further information on experimental design is available in the Nature Research Reporting Summary linked to this article.

Data availability

The high-quality reads have been deposited in the European Nucleotide Archive with accession number ERP022986. Relative abundances of taxa and functional features can be downloaded at http://arumugamlab.sund.ku.dk/SuppData/Palleja_et_al_2018_ABX/.

Received: 30 May 2018; Accepted: 28 August 2018;
Published online: 22 October 2018

References

1. Lynch, S. V. & Pedersen, O. The human intestinal microbiome in health and disease. *N. Engl. J. Med.* **375**, 2369–2379 (2016).
2. Manges, A. R. et al. Comparative metagenomic study of alterations to the intestinal microbiota and risk of nosocomial *Clostridum difficile*-associated disease. *J. Infect. Dis.* **202**, 1877–1884 (2010).
3. Ley, R. E. et al. Obesity alters gut microbial ecology. *Proc. Natl Acad. Sci. USA* **102**, 11070–11075 (2005).
4. Turnbaugh, P. J. et al. An obesity-associated gut microbiome with increased capacity for energy harvest. *Nature* **444**, 1027–1031 (2006).
5. Forslund, K. et al. Disentangling type 2 diabetes and metformin treatment signatures in the human gut microbiota. *Nature* **528**, 262–266 (2015).

6. Karlsson, F. H. et al. Gut metagenome in European women with normal, impaired and diabetic glucose control. *Nature* **498**, 99–103 (2013).
7. Qin, J. et al. A metagenome-wide association study of gut microbiota in type 2 diabetes. *Nature* **490**, 55–60 (2012).
8. Craven, M. et al. Inflammation drives dysbiosis and bacterial invasion in murine models of ileal Crohn's disease. *PLoS ONE* **7**, e41594 (2012).
9. Hsiao, E. Y. et al. Microbiota modulate behavioral and physiological abnormalities associated with neurodevelopmental disorders. *Cell* **155**, 1451–1463 (2013).
10. Konig, J. et al. Consensus report: faecal microbiota transfer—clinical applications and procedures. *Aliment. Pharmacol. Ther.* **45**, 222–239 (2017).
11. Bindels, L. B., Delzenne, N. M., Cani, P. D. & Walter, J. Towards a more comprehensive concept for prebiotics. *Nat. Rev. Gastroenterol. Hepatol.* **12**, 303–310 (2015).
12. Hemarajata, P. & Versalovic, J. Effects of probiotics on gut microbiota: mechanisms of intestinal immunomodulation and neuromodulation. *Therap. Adv. Gastroenterol.* **6**, 39–51 (2013).
13. Mikkelsen, K. H., Allin, K. H. & Knop, F. K. Effect of antibiotics on gut microbiota, glucose metabolism and body weight regulation: a review of the literature. *Diabetes Obes. Metab.* **18**, 444–453 (2016).
14. Hollis, A. & Ahmed, Z. Preserving antibiotics, rationally. *N. Engl. J. Med.* **369**, 2474–2476 (2013).
15. Nobel, Y. R. et al. Metabolic and metagenomic outcomes from early-life pulsed antibiotic treatment. *Nat. Commun.* **6**, 7486 (2015).
16. Cho, I. & Blaser, M. J. The human microbiome: at the interface of health and disease. *Nat. Rev. Genet.* **13**, 260–270 (2012).
17. Frohlich, E. E. et al. Cognitive impairment by antibiotic-induced gut dysbiosis: analysis of gut microbiota-brain communication. *Brain Behav. Immun.* **56**, 140–155 (2016).
18. Korpela, K. et al. Intestinal microbiome is related to lifetime antibiotic use in Finnish pre-school children. *Nat. Commun.* **7**, 10410 (2016).
19. Bailey, L. C. et al. Association of antibiotics in infancy with early childhood obesity. *JAMA Pediatr.* **168**, 1063–1069 (2014).
20. Saari, A., Virta, L. J., Sankilampi, U., Dunkel, L. & Saxen, H. Antibiotic exposure in infancy and risk of being overweight in the first 24 months of life. *Pediatrics* **135**, 617–626 (2015).
21. Shaw, S. Y., Blanchard, J. F. & Bernstein, C. N. Association between the use of antibiotics and new diagnoses of Crohn's disease and ulcerative colitis. *Am. J. Gastroenterol.* **106**, 2133–2142 (2011).
22. Trasande, L. et al. Infant antibiotic exposures and early-life body mass. *Int. J. Obes.* **37**, 16–23 (2013).
23. Wright, G. D. The antibiotic resistome: the nexus of chemical and genetic diversity. *Nat. Rev. Microbiol.* **5**, 175–186 (2007).
24. van Schaik, W. The human gut resistome. *Phil. Trans. R. Soc. B* **370**, 20140087 (2015).
25. Forslund, K. et al. Country-specific antibiotic use practices impact the human gut resistome. *Genome Res.* **23**, 1163–1169 (2013).
26. Rashid, M. U. et al. Determining the long-term effect of antibiotic administration on the human normal intestinal microbiota using culture and pyrosequencing methods. *Clin. Infect. Dis.* **60**, S77–S84 (2015).
27. Zaura, E. et al. Same exposure but two radically different responses to antibiotics: resilience of the salivary microbiome versus long-term microbial shifts in feces. *mBio* **6**, e01693-15 (2015).
28. Reijnders, D. et al. Effects of gut microbiota manipulation by antibiotics on host metabolism in obese humans: a randomized double-blind placebo-controlled trial. *Cell Metab.* **24**, 63–74 (2016).
29. Abeles, S. R. et al. Microbial diversity in individuals and their household contacts following typical antibiotic courses. *Microbiome* **4**, 39 (2016).
30. Raymond, F. et al. The initial state of the human gut microbiome determines its reshaping by antibiotics. *ISME J.* **10**, 707–720 (2016).
31. Mikkelsen, K. H. et al. Effect of antibiotics on gut microbiota, gut hormones and glucose metabolism. *PLoS ONE* **10**, e0142352 (2015).
32. Houben, A. J. et al. Selective decontamination of the oropharynx and the digestive tract, and antimicrobial resistance: a 4 year ecological study in 38 intensive care units in the Netherlands. *J. Antimicrob. Chemother.* **69**, 797–804 (2014).
33. Nielsen, H. B. et al. Identification and assembly of genomes and genetic elements in complex metagenomic samples without using reference genomes. *Nat. Biotechnol.* **32**, 822–828 (2014).
34. Sunagawa, S. et al. Metagenomic species profiling using universal phylogenetic marker genes. *Nat. Methods* **10**, 1196–1199 (2013).
35. Consortium, H. M. P. Structure, function and diversity of the healthy human microbiome. *Nature* **486**, 207–214 (2012).
36. Voigt, A. Y. et al. Temporal and technical variability of human gut metagenomes. *Genome Biol.* **16**, 73 (2015).
37. Talukdar, P. K., Olguin-Araneda, V., Alnoman, M., Paredes-Sabja, D. & Sarker, M. R. Updates on the sporulation process in *Clostridium* species. *Res. Microbiol.* **166**, 225–235 (2015).
38. Maier, L. et al. Extensive impact of non-antibiotic drugs on human gut bacteria. *Nature* **555**, 623–628 (2018).
39. Li, J. et al. An integrated catalog of reference genes in the human gut microbiome. *Nat. Biotechnol.* **32**, 834–841 (2014).
40. Kultima, J. R. et al. MOCAT2: a metagenomic assembly, annotation and profiling framework. *Bioinformatics* **32**, 2520–2523 (2016).
41. Jia, B. et al. CARD 2017: expansion and model-centric curation of the comprehensive antibiotic resistance database. *Nucleic Acids Res.* **45**, D566–D573 (2017).
42. Gibson, M. K., Forsberg, K. J. & Dantas, G. Improved annotation of antibiotic resistance determinants reveals microbial resistomes cluster by ecology. *ISME J.* **9**, 207–216 (2015).
43. Queenan, A. M. & Bush, K. Carbapenemases: the versatile β-lactamases. *Clin. Microbiol. Rev.* **20**, 440–458 (2007).
44. Werner, G., Strommenger, B. & Witte, W. Acquired vancomycin resistance in clinically relevant pathogens. *Future Microbiol.* **3**, 547–562 (2008).
45. Damier-Piolle, L., Magnet, S., Brémont, S., Lambert, T. & Courvalin, P. AdeIJK, a resistance-nodulation-cell division pump effluxing multiple antibiotics in *Acinetobacter baumannii*. *Antimicrob. Agents Chemother.* **52**, 557–562 (2008).
46. Hou, P. F., Chen, X. Y., Yan, G. F., Wang, Y. P. & Ying, C. M. Study of the correlation of imipenem resistance with efflux pumps AdeABC, AdeIJK, AdeDE and AbeM in clinical isolates of *Acinetobacter baumannii*. *Chemotherapy* **58**, 152–158 (2012).
47. Kanehisa, M. et al. Data, information, knowledge and principle: back to metabolism in KEGG. *Nucleic Acids Res.* **42**, D199–D205 (2014).
48. Pu, Y. et al. Enhanced efflux activity facilitates drug tolerance in dormant bacterial cells. *Mol. Cell* **62**, 284–294 (2016).
49. Winter, S. E. et al. Gut inflammation provides a respiratory electron acceptor for *Salmonella*. *Nature* **467**, 426–429 (2010).
50. Winter, S. E. et al. Host-derived nitrate boosts growth of *E. coli* in the inflamed gut. *Science* **339**, 708–711 (2013).
51. Rivera-Chávez, F. et al. Depletion of butyrate-producing *Clostridia* from the gut microbiota drives an aerobic luminal expansion of *Salmonella*. *Cell Host Microbe* **19**, 443–454 (2016).
52. Zhu, W. et al. Precision editing of the gut microbiota ameliorates colitis. *Nature* **553**, 208–211 (2018).
53. Driscoll, T. et al. Integration and visualization of host-pathogen data related to infectious diseases. *Bioinformatics* **27**, 2279–2287 (2011).
54. Rutherford, S. T. & Bassler, B. L. Bacterial quorum sensing: its role in virulence and possibilities for its control. *Cold Spring Harb. Perspect. Med.* **2**, a012427 (2012).
55. Buffie, C. G. & Pamer, E. G. Microbiota-mediated colonization resistance against intestinal pathogens. *Nat. Rev. Immunol.* **13**, 790–801 (2013).
56. Kassam, Z., Lee, C. H., Yuan, Y. & Hunt, R. H. Fecal microbiota transplantation for *Clostridium difficile* infection: systematic review and meta-analysis. *Am. J. Gastroenterol.* **108**, 500–508 (2013).
57. Finegold, S. M. et al. Gastrointestinal microflora studies in late-onset autism. *Clin. Infect. Dis.* **35**, S6–S16 (2002).
58. Song, Y., Liu, C. & Finegold, S. M. Real-time PCR quantitation of *Clostridia* in feces of autistic children. *Appl. Environ. Microbiol.* **70**, 6459–6465 (2004).
59. Luna, R. A. et al. Distinct microbiome-neuroimmune signatures correlate with functional abdominal pain in children with autism spectrum disorder. *Cell. Mol. Gastroenterol. Hepatol.* **3**, 218–230 (2017).
60. Ren, Z. et al. Intestinal microbial variation may predict early acute rejection after liver transplantation in rats. *Transplantation* **98**, 844–852 (2014).
61. Le Chatelier, E. et al. Richness of human gut microbiome correlates with metabolic markers. *Nature* **500**, 541–546 (2013).
62. Rao, S., Kupfer, Y., Pagala, M., Chapnick, E. & Tessler, S. Systemic absorption of oral vancomycin in patients with *Clostridium difficile* infection. *Scand. J. Infect. Dis.* **43**, 386–388 (2011).
63. Rohrbaugh, T. M., Anolik, R., August, C. S., Serota, F. T. & Koch, P. A. Absorption of oral aminoglycosides following bone marrow transplantation. *Cancer* **53**, 1502–1506 (1984).
64. Craig, W. A. The pharmacology of meropenem, a new carbapenem antibiotic. *Clin. Infect. Dis.* **24**, S266–S275 (1997).
65. *IHMS_SOP 07 V2: Standard Operating Procedure for Fecal Samples DNA Extraction* Protocol H INRA (IHMS, 2015); http://www.microbiome-standards.org/index.php?id=254
66. Kultima, J. R. et al. MOCAT: a metagenomics assembly and gene prediction toolkit. *PLoS ONE* **7**, e47656 (2012).
67. Yutin, N. & Galperin, M. Y. A genomic update on clostridial phylogeny: Gram-negative spore formers and other misplaced clostridia. *Environ. Microbiol.* **15**, 2631–2641 (2013).
68. Li, H. & Durbin, R. Fast and accurate short read alignment with Burrows-Wheeler transform. *Bioinformatics* **25**, 1754–1760 (2009).
69. Liu, B. & Pop, M. ARDB—antibiotic resistance genes database. *Nucleic Acids Res.* **37**, D443–D447 (2009).
70. Edgar, R. C. Search and clustering orders of magnitude faster than BLAST. *Bioinformatics* **26**, 2460–2461 (2010).

71. Lovell, D., Pawlowsky-Glahn, V., Egozcue, J. J., Marguerat, S. & Bähler, J. Proportionality: a valid alternative to correlation for relative data. *PLoS Comput. Biol.* **11**, e1004075 (2015).
72. Weiss, S. et al. Normalization and microbial differential abundance strategies depend upon data characteristics. *Microbiome* **5**, 27 (2017).
73. Aitchison, J. The statistical analysis of compositional data. *J. R. Stat. Soc. Ser. B* **44**, 139–177 (1982).
74. Palleja, A. et al. Roux-en-Y gastric bypass surgery of morbidly obese patients induces swift and persistent changes of the individual gut microbiota. *Genome Med.* **8**, 67 (2016).

Acknowledgements

This work was funded by an international alliance grant from The Novo Nordisk Foundation Center for Basic Metabolic Research, which is an independent Research Center at the University of Copenhagen partially funded by an unrestricted donation from the Novo Nordisk Foundation (grant no. NNF10CC1016515). Our work was also funded by the TARGET research initiative (Danish Strategic Research Council [0603–00484B]), the Danish Diabetes Academy supported by the Novo Nordisk Foundation, the Danish Council for Independent Research (Medical Sciences), and the Danish Diabetes Association. S.K.F. was funded by FP7 METACARDIS HEALTH-F4-2012-305312.

Author contributions

O.P., T.H. and F.K.K. devised the study protocol. M.F.N. participated in the protocol design and application and in the participant recruitment and selection. K.H.M. performed sample collections and carried out patient phenotyping. K.H.A. supervised the microbial DNA extraction. S.L., C.Z., J.W., Q.F. and H.Y. performed shotgun metagenomics sequencing and taxonomic profiling. P.T.P., L.P.C. and M.A. estimated IGC gene profiles. H.B.N. generated the MGS groups based on IGC. A.P., S.K.F. and A.K. designed and performed the data analysis. M.A., T.H., P.B. and O.P. supervised the data analysis. A.P., S.K.F., K.H.M. and M.A. wrote the paper. K.H.A., T.N., T.H.H., A.K., H.B.N., J.W., A.T., P.B., T.V., F.K.K., T.H. and O.P. revised the paper. All authors contributed to data interpretation, discussion and editing of the paper. All authors read and approved the final manuscript.

Competing interests

The authors declare no competing interests.

Additional information

Supplementary information is available for this paper at https://doi.org/10.1038/s41564-018-0257-9.

Reprints and permissions information is available at www.nature.com/reprints.

Correspondence and requests for materials should be addressed to F.K.K. or M.A. or O.P.

Publisher's note: Springer Nature remains neutral with regard to jurisdictional claims in published maps and institutional affiliations.